

# Aromatic C<sub>20</sub>F<sub>20</sub> cage and its endohedral complexes X@C<sub>20</sub>F<sub>20</sub> (X = H<sup>-</sup>, F<sup>-</sup>, Cl<sup>-</sup>, Br<sup>-</sup>, H, He)

Cai-Yun Zhang · Hai-Shun Wu · Haijun Jiao

Received: 27 July 2006 / Accepted: 13 December 2006 / Published online: 26 January 2007  
© Springer-Verlag 2007

**Abstract** The structure and stability of endohedral X@C<sub>20</sub>F<sub>20</sub> complexes (X = H<sup>-</sup>, F<sup>-</sup>, Cl<sup>-</sup>, Br<sup>-</sup>, H, He) have been computed at the B3LYP level of theory. All complexes in I<sub>h</sub> symmetry were found to be energy minimum structures. H<sup>-</sup>@C<sub>20</sub>F<sub>20</sub> and F<sup>-</sup>@C<sub>20</sub>F<sub>20</sub> complexes have negative inclusion energies, while other complexes have positive inclusion energies. Similarity between C<sub>20</sub>F<sub>20</sub> and C<sub>20</sub>H<sub>20</sub> has been found for X = H and He. On the basis of the computed nucleus independent chemical shift values at the cage center, both C<sub>20</sub>F<sub>20</sub> and C<sub>20</sub>H<sub>20</sub> are aromatic.

**Keywords** C<sub>20</sub>F<sub>20</sub> · DFT · Aromaticity · Endohedral complexes

## Introduction

Dodecahedrane (C<sub>20</sub>H<sub>20</sub>) [1] is an aesthetic molecule with unusually high symmetry (I<sub>h</sub>) and provides the opportunity for fascinating chemistry [2–4]. Apart from the chemistry of the outer cage, the encapsulation of various guest atoms and ions has been explored theoretically [5–10]. The first experimental example is the encapsulation of He into

C<sub>20</sub>H<sub>20</sub> (He@C<sub>20</sub>H<sub>20</sub>) [11]. In addition, the endohedral complexes of small hydrocarbon cages (C<sub>4</sub>H<sub>4</sub>, C<sub>8</sub>H<sub>8</sub>, C<sub>8</sub>H<sub>14</sub>, C<sub>10</sub>H<sub>16</sub>, C<sub>12</sub>H<sub>12</sub> and C<sub>16</sub>H<sub>16</sub>) have also been investigated [12]. More recently, the endohedral complexes of Si<sub>20</sub>H<sub>20</sub> (X@Si<sub>20</sub>H<sub>20</sub>) have been studied and significant charge transfer from X into the cage has been observed [13, 14].

For encapsulating anions, it is conceptual to have cages with partially positive charged inner sides. An appropriate candidate for this purpose is perfluorododecahedrane (C<sub>20</sub>F<sub>20</sub>), due to the different electronegativities of carbon and fluorine. Although the existence of C<sub>20</sub>F<sub>20</sub> has been reported [4], the best information is computational [15]. Indeed, perfluoroalkanes have exceptional chemical and physical properties compared to their parent hydrocarbons. For example, hydrocarbons have been computed to have negative adiabatic electron affinity [16], and corresponding perfluorohydrocarbons have substantial adiabatic electron affinities and the ability to bind an additional electron [17–22]. Similarly, C<sub>20</sub>H<sub>20</sub> has been predicted to have negative adiabatic electron affinity (−0.71 eV) [9]. i.e., it does not readily attract an electron. Based on these properties, C<sub>20</sub>F<sub>20</sub> is expected to have large electron affinity and therefore significantly stabilize capsulated spherical anions. Here, we report the structure and stability of endohedral X@C<sub>20</sub>F<sub>20</sub> complexes (X = H<sup>-</sup>, F<sup>-</sup>, Cl<sup>-</sup>, Br<sup>-</sup>, H and He) at the B3LYP level of density functional theory.

## Methods

All calculations were carried out using the Gaussian 03 software package [23]. Guest anions or atoms were placed at the cage centers. All structures were optimized at the B3LYP/6-31G\* level of density functional theory, and the corresponding frequency calculations at the same level

C.-Y. Zhang · H.-S. Wu  
School of Chemistry and Materials Science,  
Shanxi Normal University,  
Linfen 041004, China

H.-S. Wu  
e-mail: wuhs@dns.sxnu.edu.cn

H. Jiao (✉)  
Leibniz-Institut für Katalyse e.V. an der Universität Rostock,  
Albert-Einstein-Strasse 29a,  
18059 Rostock, Germany  
e-mail: haijun.jiao@catalysis.de

identify the optimized structures as energy minima without imaginary frequencies. Atomic charges were calculated using natural bond orbital analysis [24]. Single-point energies were calculated at the B3LYP/6-311+G\*\* level with the B3LYP/6-31G\* optimized geometries.

The inclusion energy ( $E_{\text{inc}}$ ) is defined as the difference between  $\text{X}@C_{20}\text{F}_{20}$  and the sum of  $C_{20}\text{F}_{20}$  and  $\text{X}$ . On this basis, a negative  $E_{\text{inc}}$  means favored encapsulation, while a positive  $E_{\text{inc}}$  means disfavored encapsulation. The deformation energy ( $E_{\text{def}}$ ) is defined as the difference between the free optimized  $C_{20}\text{F}_{20}$  cage and the cage with encapsulation from single-point energy calculation. For estimating the degree of electron delocalization of  $C_{20}\text{F}_{20}$  and  $C_{20}\text{F}_{20}^-$ , nucleus independent chemical shift (NICS) [25–27], the negative of the absolute shielding at the cage center, was calculated using the gauge-independent atomic orbital (GIAO) [28] method and B3LYP/6-31G\* geometry.

## Results and discussion

### $C_{20}\text{F}_{20}$ and $C_{20}\text{F}_{20}^-$

Like  $C_{20}\text{H}_{20}$ , the  $I_h$ -symmetrical  $C_{20}\text{F}_{20}$  (Fig. 1) is an energy minimum. The C–C bond length is 1.562 Å and the C–X distance (X for the cage center) is 2.188 Å; these parameters are close to those of  $C_{20}\text{H}_{20}$  (1.557 and 2.181 Å, respectively). In  $C_{20}\text{F}_{20}$ , the polarized C–F bonds constitute an approximate  $C^{\delta+}\text{F}^{\delta-}$  double electric layer due to the negatively charged outer F shell ( $\delta_F=-0.318$ ) and the positively charged inner C shell is ( $\delta_C=+0.318$ ). Although there is also a double electric layer in  $C_{20}\text{H}_{20}$ , the inner C shell is negatively charged ( $\delta_C=-0.248$ ) and the outer H layer is positively charged ( $\delta_H=0.248$ ); this is just the opposite of  $C_{20}\text{F}_{20}$ .

As shown in Fig. 2, the  $C_{20}\text{F}_{20}$  cage structure has degenerate HOMOs ( $H_u$ ); removal of one electron from the HOMO will lead to Jahn-Teller distortion. However, the corresponding LUMO ( $A_g$ ) is non-degenerate and distributes fully around the cage center, therefore the cage is able to host one additional electron into the LUMO without lowering the high symmetry. Indeed,  $C_{20}\text{F}_{20}^-$  cage in  $I_h$  symmetry is an energy minimum on the B3LYP/6-31G\* potential energy surface. Compared to  $C_{20}\text{F}_{20}$ , the C–C bond length of  $C_{20}\text{F}_{20}^-$  becomes shorter, while that of C–F becomes longer (1.562/1.358 vs 1.550/1.379 Å, respectively). Compared also to  $C_{20}\text{F}_{20}$ , the negative charge is distributed over both carbon and fluorine in  $C_{20}\text{F}_{20}^-$ , carbon becomes less positively charged (0.318 vs 0.299), and fluorine becomes more negatively charged (-0.318 vs -0.349).

The ability of  $C_{20}\text{F}_{20}$  to host one additional electron is reflected by the computed electron affinity. At B3LYP/6-311+G\*/B3LYP/6-31G\*, the calculated electron affinity (or inclusion energy of one electron) is 3.66 eV for  $C_{20}\text{F}_{20}^-$ , which is also stronger than that of an F atom (3.49 eV) at the same level, compared with the experimental value (3.45 eV) [29]. This good agreement validates the computational method. Therefore, adding an electron does not lower the symmetry, and this novel structural model of  $C_{20}\text{F}_{20}$  can stabilize the encapsulated spherical anions significantly.

The degree of delocalization of the added electron in the LUMO can be tested by the computed NICS, which is a simple and efficient criterion of aromaticity. For  $C_{20}\text{F}_{20}$ , the computed NICS is -7.7 ppm, indicating the partial delocalization of the skeleton electrons of the C shell; this is because that the inner carbon shell is positively charged. For comparison, the NICS value of  $C_{20}\text{H}_{20}$  is +1.7 ppm at the same level. For  $C_{20}\text{F}_{20}^-$ , the computed NICS value is -10.5 ppm, i.e., more negative than that of  $C_{20}\text{F}_{20}$ , revealing the increased delocalization effect of the added

**Fig. 1** Endohedral  $\text{X}@C_{20}\text{F}_{20}$  complex

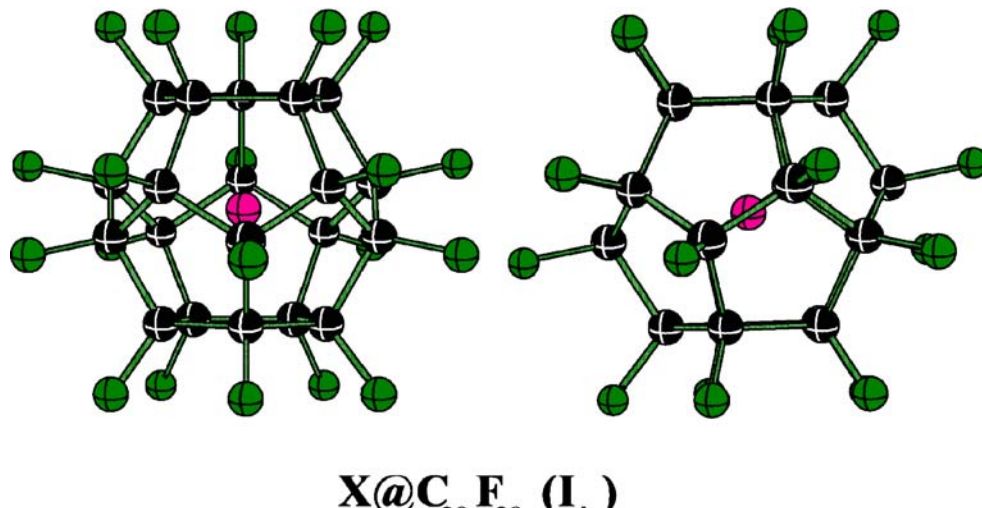
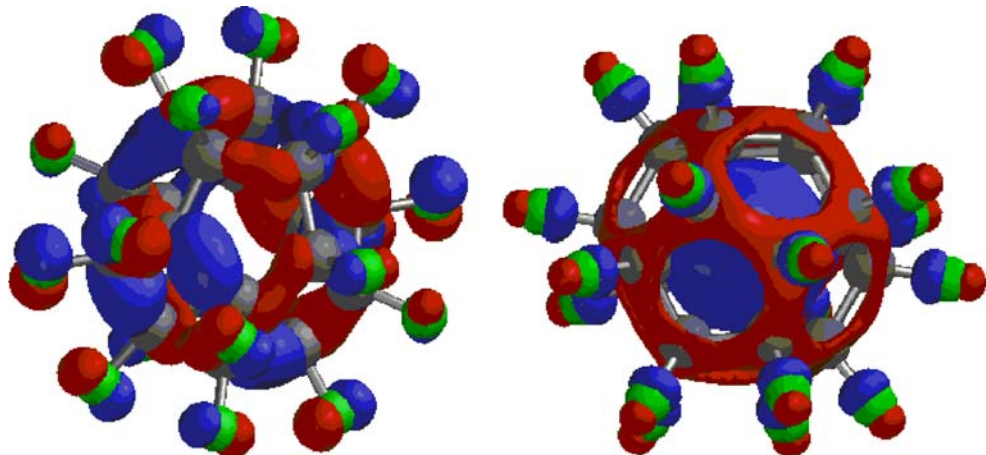


**Fig. 2** The HOMO ( $H_u$ , left) and LUMO ( $A_g$ , right) orbitals of  $C_{20}F_{20}$



electron. It is also interesting to note that the NICS values of  $C_{20}F_{20}$  and  $C_{20}F_{20}^-$  are close to that (-8.9 ppm) of benzene at the ring center [26]. Therefore, both  $C_{20}F_{20}$  and  $C_{20}F_{20}^-$  can be considered as aromatic systems. That  $C_{20}F_{20}$  is aromatic is further evidenced by the calculated diamagnetic susceptibility exaltation of -22.5 ppm.cgs [the diamagnetic susceptibility exaltation is evaluated on the basis of the equation,  $20\ CF(CH_3)_3 - 30\ C_2H_6 = C_{20}F_{20}$ , at the B3LYP/6-31G\* level with the CSGT method]. The computed diamagnetic susceptibility (ppm cgs) is -41.1 for  $CF(CH_3)_3$ , -19.9 for  $C_2H_6$ , and -247.5 for  $C_{20}F_{20}$ . For comparison, benzene has a diamagnetic susceptibility exaltation of -14.5 ppm cgs (for the background and methodology for the diamagnetic susceptibility exaltation calculation, see [30]), [31].

#### $X@C_{20}F_{20}$ ( $X = H^-, F^-, Cl^-, Br^-$ )

Since  $C_{20}F_{20}$  can accept one additional electron to form the stable  $C_{20}F_{20}^-$  without lowering the symmetry, we were interested in the structure and stability of the endohedral

complex of  $X@C_{20}F_{20}$  ( $X = H^-, F^-, Cl^-, Br^-$ ). At B3LYP/6-31G\*, all complexes in  $I_h$  symmetry are energy minima. As shown in Table 1, both  $H^-$  and  $F^-$  have negative  $E_{inc}$ , indicating thermodynamic favorability. In contrast,  $Cl^-$  and  $Br^-$  have positive  $E_{inc}$ , showing the difficulty of encapsulation, as well as showing that the decreased  $E_{inc}$  increases with increasing ion radii. In addition, we have also computed the deformation energy of the cage. As shown in Table 1, deformation energy ( $E_{def}$ ) increases with ion radii, but it contributes only a small fraction to  $E_{inc}$ .

As shown in Table 1, the C–C bond length increases along  $X = H^-, F^-, Cl^-, Br^-$ , while the C–F bond length decreases accordingly. It is also interesting to note that the inclusion energy for  $X = H^-$  and  $F^-$  is even stronger than that of one electron (-130.9 and -93.5 vs -84.3 kcal mol<sup>-1</sup>). As shown below, this is associated with the degree of charge transfer and the electrostatic interaction between the cage inner and the partially charged guests. In addition, we have also computed the basis set superposition error (BSSE) [32]. As given in Table 1, the BSSE for  $X = He$  and  $H$  are negligible (0.7 and 0.8 kcal mol<sup>-1</sup>, respectively), while those

**Table 1** Total electronic energies ( $E_{tot}$ , au), bond distances (Å), inclusion energies ( $E_{inc}$ , kcal mol<sup>-1</sup>), and cage deformation energies ( $E_{def}$ , kcal mol<sup>-1</sup>). BSSE Basis set superposition error

$X@C_{20}F_{20}$	$E_{tot}^a$	$E_{tot}^b$	$R_{X-C}^a$	$R_{C-C}^a$	$R_{C-F}^a$	$E_{inc}^d$	BSSE <sup>e</sup>	$E_{def}^f$
$C_{20}F_{20}$	-2758.70603	-2759.55858	(2.188) <sup>c</sup>	1.562	1.358			
$C_{20}F_{20}^-$	-2758.79783	-2759.69295	(2.172) <sup>c</sup>	1.550	1.379	-84.3		6.2
$H^-@C_{20}F_{20}$	-2759.39750	-2760.28507	2.180	1.556	1.374	-130.9	17.1	3.8
$F^-@C_{20}F_{20}$	-2858.67980	-2859.59631	2.201	1.571	1.370	-93.5	6.7	2.7
$Cl^-@C_{20}F_{20}$	-3218.70902	-3219.57975	2.260	1.613	1.368	177.3	4.8	22.6
$Br^-@C_{20}F_{20}$	-5330.13414	-5333.29881	2.283	1.629	1.369	312.2	4.2	38.3
$He@C_{20}F_{20}$	-2761.56645	-2762.42480	2.199	1.570	1.356	29.4	0.7	<0.1
$H@C_{20}F_{20}$	-2759.16532	-2760.01976	2.197	1.568	1.358	30.6	0.8	<0.1

<sup>a</sup> At B3LYP/6-31G\*

<sup>b</sup> At B3LYP/6-311+G\*\*//B3LYP/6-31G\*

<sup>c</sup> Distance to cage center

<sup>d</sup> Inclusion energy;  $E_{inc} = E(X@C_{20}F_{20}) - [E(X) + E(C_{20}F_{20})]$

<sup>e</sup> BSSE at B3LYP/6-311+G\*\*//B3LYP/6-31G\*

<sup>f</sup> Cage deformation energy;  $E_{def} = E(C_{20}F_{20})/(strain) - E(C_{20}F_{20})$

**Table 2** Calculated natural atomic charge ( $q$ ) and its change ( $\Delta q$ )

Complex	$q_C$	$q_F$	$q_X$	$\Delta q_X$
$C_{20}F_{20}$	+0.318	-0.318		
$C_{20}F_{20}^-$	+0.299	-0.349		
$H^-@C_{20}F_{20}$	+0.317	-0.348	-0.377	+0.623
$F^-@C_{20}F_{20}$	+0.328	-0.351	-0.547	+0.453
$Cl^-@C_{20}F_{20}$	+0.295	-0.350	+0.107	+1.107
$Br^-@C_{20}F_{20}$	+0.275	-0.350	+0.499	+1.499
$He@C_{20}F_{20}$	+0.315	-0.319	+0.060	+0.060
$H@C_{20}F_{20}$	+0.311	-0.317	+0.120	+0.120

for  $X = F^-$ ,  $Cl^-$  and  $Br^-$  are also small (6.8, 4.8 and 4.2 kcal mol $^{-1}$ , respectively). The largest BSSE is found for  $X = H^-$  (17.1 kcal mol $^{-1}$ ). Nevertheless, BSSE correction does not change the order of the inclusion energies.

The computed natural charges in Table 2 of the encapsulated guests reveal the significant charge transfer between cage and guest. For  $X = H^-$  and  $F^-$ , the guest has partially negative charge (-0.377 and -0.547, respectively), and this might explain their much stronger inclusion energies than that of one electron. This is because, apart from the charge transfer, the partially negative charge guest interacts with the positively charged inner side of the cage. For  $X = Cl^-$  and  $Br^-$ , however, the guest is slightly positively charged (+0.107 and +0.499, respectively), indicating the transfer of more than one charge unit from guest to host. This might explain the rather positive inclusion energies. All these show the oxidation potential of  $C_{20}F_{20}$ .

#### $X@C_{20}F_{20}$ ( $X = H$ , He)

On the basis of the results for anion encapsulation, it is interesting to compare that for hydrogen atoms and helium atoms. For  $X = H$  and He, the encapsulated complexes have  $I_h$  symmetry, despite the radical character of the hydrogen atom as in the case of  $C_{20}F_{20}^-$ . Compared to  $C_{20}F_{20}$ , there are no significant changes of C–C and C–F bond lengths in  $H@C_{20}F_{20}$  and  $He@C_{20}F_{20}$ , and it should also be noted that the cage deformation energies are smaller than 0.1 kcal mol $^{-1}$ . The computed inclusion energies are positive (30.6 and 29.4 kcal mol $^{-1}$ ) and smaller than those reported for  $H@C_{20}H_{20}$  (35.8 kcal mol $^{-1}$ ) [9] and  $He@C_{20}H_{20}$  (33.8 kcal mol $^{-1}$  [8] and 37.9 kcal mol $^{-1}$  [9]).

#### Conclusion

The structure and stability of the  $C_{20}F_{20}$  cage and its radical anion  $C_{20}F_{20}^-$ , as well as the endohedral complexes  $X@C_{20}F_{20}$  have been computed at the B3LYP density functional level of theory. As expected,  $C_{20}F_{20}$  has a double

electric layer, in which the inner carbon shell is positively charged, and the outer fluorine shell is negatively charged. Due to the spherically distributed LUMO,  $C_{20}F_{20}$  can host one additional electron without lowering its  $I_h$ -symmetry. On the basis of the computed NICS values,  $C_{20}F_{20}$  and  $C_{20}F_{20}^-$  can be considered as aromatic systems.

The double electric layer structure of  $C_{20}F_{20}$  provides the possibility to host guest anions as energy minimum structures,  $X@C_{20}F_{20}$  ( $X = H^-$ ,  $F^-$ ,  $Cl^-$ ,  $Br^-$ ), in which both  $H^-@C_{20}F_{20}$  and  $F^-@C_{20}F_{20}$  with partially negatively charged guests have negative inclusion energies, while  $Cl^-@C_{20}F_{20}$  and  $Br^-@C_{20}F_{20}$  with partially positively charged guests have positive inclusion energies. These energies are associated with the strong charge transfer between cage and guest, and their electrostatic interaction.

Similar results for  $X = H$  and He have been found for the endohedral complexes of  $C_{20}F_{20}$  and  $C_{20}H_{20}$ . They have  $I_h$ -symmetry as energy minimum structures; however, those of  $C_{20}F_{20}$  have somewhat smaller inclusion energies than those of  $C_{20}H_{20}$ .

**Acknowledgments** This work was supported by the Special Funds of the Shanxi Normal University and the National Nature Science Foundation of China (20673070).

#### References

1. Paquette LA (1989) Chem Rev 89:1051–1065
2. Paquette LA (1990) The [n] peristyrene-polyhedrane connection. In: Olah GA (ed) Cage hydrocarbons. Wiley, New York, pp 313–352
3. Fessner WD, Prinzbach H (1990) The pagodane route to dodecahedrane. In: Olah GA (ed) Cage hydrocarbons. Wiley, New York, pp 353–405
4. Prinzbach H, Weber K (1994) Angew Chem Int Ed Engl 33:2239–2258
5. Schulman JM, Disch RL (1978) J Am Chem Soc 100:5677–5681
6. Dixon DA, Deerfield D, Graham GD (1981) Chem Phys Lett 78:161–164
7. Chen Z, Jiao H, Bühl M, Hirsch A, Thiel W (2001) Theor Chem Acc 106:352–363
8. Jimenez-Vazquez HA, Tamariz J, Cross RJ (2001) J Phys Chem A 105:1315–1319
9. Moran D, Stahl F, Jemmis ED, Schaefer III HF, Schleyer PvR (2002) J Phys Chem A 106:5144–5154
10. Chen Z, Jiao H, Moran D, Hirsch A, Thiel W, Schleyer PvR (2003) J Phys Chem A 107:2075–2079
11. Cross RJ, Saunders M, Prinzbach H (1999) Org Lett 1:1479–1481
12. Moran D, Woodcock HL, Chen Z, Schaefer III HF, Schleyer PvR (2003) J Am Chem Soc 125:11442–11451
13. Pichierri F, Kumar V, Kawazoe Y (2005) Chem Phys Lett 406:341–344
14. Zhang CY, Wu HS, Jiao H (2005) Chem Phys Lett 410:457–461
15. Cioslowski J, Edgington L, Stefanov BB (1995) J Am Chem Soc 117:10381–10384
16. Yan G, Brinkmann NR, Schaefer III HF (2003) J Phys Chem A 107:9479–9485
17. Beck CM, Burdeniuc J, Crabtree RH, Rheingold AL, Yap GP (1998) Inorg Chem Acta 270:559–562

18. Alkorta I, Rozas I, Elguero J (2002) *J Am Chem Soc* 124:8593–8598
19. Xie Y, Schaefer III HF, Cotton FA (2003) *Chem Commun* 102–103
20. Li Q, Feng X, Xie Y, Schaefer III HF (2004) *J Phys Chem A* 108:7071–7078
21. Li Q, Feng X, Xie Y, Schaefer III HF (2005) *J Phys Chem A* 109:1454–1457
22. Paul A, Wannere CS, Kasalova V, Schleyer PvR, Schaefer III HF (2005) *J Am Chem Soc* 127:15457–15469
23. Frisch MJ, Trucks GW, Schlegel HB, Scuseria GE, Robb MA, Cheeseman JR, Montgomery Jr JA, Vreven T, Kudin KN, Burant JC, Millam JM, Iyengar SS, Tomasi J, Barone V, Mennucci B, Cossi M, Scalmani G, Rega N, Petersson GA, Nakatsuji H, Hada M, Ehara M, Toyota K, Fukuda R, Hasegawa J, Ishida M, Nakajima T, Honda Y, Kitao O, Nakai H, Klene M, Li X, Knox JE, Hratchian HP, Cross JB, Bakken V, Adamo C, Jaramillo J, Gomperts R, Stratmann RE, Yazyev O, Austin AJ, Cammi R, Pomelli C, Ochterski JW, Ayala PY, Morokuma K, Voth GA, Salvador P, Dannenberg JJ, Zakrzewski VG, Dapprich S, Daniels AD, Strain MC, Farkas O, Malick DK, Rabuck AD, Raghavachari K, Foresman JB, Ortiz JV, Cui Q, Baboul AG, Clifford S, Cioslowski J, Stefanov BB, Liu G, Liashenko A, Piskorz P, Komaromi I, Martin RL, Fox DJ, Keith T, Al-Laham MA, Peng CY, Nanayakkara A, Challacombe M, Gill PMW, Johnson B, Chen W, Wong MW, Gonzalez C, Pople JA (2000) Gaussian 03, Revision C.02. Gaussian Inc, Wallingford CT
24. Reed AE, Curtiss LA, Weinhold F (1988) *Chem Rev* 88:899–926
25. Schleyer PvR, Maerker C, Dransfeld A, Jiao H, van Eikema Hommes NJR (1996) *J Am Chem Soc* 118:6317–6318
26. Schleyer PvR, Jiao H, van Eikema Hommes NJR, Malkin VG, Malkina OL (1997) *J Am Chem Soc* 119:12669–12670
27. Schleyer PvR, Manoharan M, Wang ZX, Kiran B, Jiao H, Puchta R, van Eikema Hommes NJR (2001) *Org Lett* 3:2465–2468
28. Wolinski K, Hinton JF, Pulay P (1990) *J Am Chem Soc* 112:8251–8260
29. Greenwood NN, Earnshaw A (1990) *Chemie der elemente*. VCH, Weinheim
30. Jiao H, Nagelkerke R, Kurtz HA, Williams RV, Borden WT, Schleyer PvR (1997) *J Am Chem Soc* 119:5921–5929
31. Jiao H, Schleyer PvR, Mo Y, McAllister MA, Tidwell TT (1997) *J Am Chem Soc* 119:7075–7083
32. Simon S, Duran M, Dannenberg JJ (1996) *J Chem Phys* 105:11024–11031